InSAR Studies of Alaskan Volcanoes

Zhong Lu
U.S. Geological Survey (USGS), EROS Data Center, SAIC
47914 252nd Street, Sioux Falls, SD 57198
lu@usgs.gov; http://edc.usgs.gov/Geo_Apps

Chuck Wicks
USGS, Earthquake & Volcano Hazards Programs
345 Middlefield Rd., Menlo Park, CA 94025
cwicks@usgs.gov

Dan Dzurisin,
USGS, Cascades Volcano Observatory
1300 S.E. Cardinal Court, Suite 100, Vancouver, WA 98683-9589
dzurisin@usgs.gov

John Power
USGS, Alaska Volcano Observatory
4200 University Drive, Anchorage, AK 99508
jpower@usgs.gov

Abstract: Interferometric synthetic aperture radar (InSAR) is a remote sensing technique capable of measuring ground surface deformation with sub-centimeter precision and spatial resolution in tens-of-meters over a large region. This paper highlights our on-going investigations of Aleutian volcanoes with SAR images acquired from European ERS-1 and ERS-2, Canadian Radarsat-1, and Japanese JERS-1 satellites.

1. New Trident Volcano

The first application of InSAR exploring study surface deformation over the Aleutians was for New Trident volcano (Fig. 1) that last erupted in 1963. An ERS-1 interferogram indicated about 7-9 cm of uplift from 1993 to 1995 [1]. Numerical modeling suggested inflation of a magma body located about 2 km beneath the volcano. Shortly thereafter, Alaska Volcano Observatory (AVO) geologists noted signs of dome-like uplift and fumarolic activity at New Trident (J. Freymueller, pers. comm., 1997).

2. Okmok Volcano

Okmok volcano (Fig. 1), a broad shield topped with a 10-km-wide caldera, produced blocky basaltic flows during relatively large effusive eruptions in 1945, 1958 and 1997 [2]. Multiple InSAR images mapped 1) the surface inflation of more than 18 cm during 1992-1995 and subsidence of 1-2 cm during 1995-1996 prior to the 1997 eruption, 2) more than 140 cm of surface deflation during the 1997 eruption (Fig. 2a), and 3) 5-15 cm/year inflation during 1997-2003 after the 1997 eruption. Numerical modeling suggested the magma reservoir responsible for the observed deformation resided at a depth of about 3 km beneath the center of the caldera and about 5 km away from the eruptive vent. This example demonstrates how InSAR is capable of measuring pre-eruptive, co-eruptive, and post-eruptive deformation in the sub-arctic environment [3, 4, 5, 6].

3. Akutan Volcano

Akutan volcano (Fig. 1), the second most active volcano in Alaska, was shaken by an intense earthquake swarm accompanied by extensive ground cracking but no eruption of the volcano. Both L-band JERS-1 and C-band ERS-1/2 InSAR images show uplift as much as 60 cm on the western part of the island associated with the swarm. The JERS interferogram (Fig. 2b), displaying greater coherence, especially in areas with loose surface material or thick vegetation, also shows subsidence of similar magnitude on the eastern part of the island, and displacements along faults reactivated during the swarm. The axis of uplift and subsidence strikes about N70°W and is roughly parallel 1) to a zone of fresh cracks on the volcano's northwest flank, 2) to normal faults that cut the island, and 3) to the inferred maximum compressive stress direction. Both before and after the swarm, the northwest flank uplifted 5-20 mm/year relative to the southwest flank, probably by magma intrusion. This

example demonstrates that InSAR can provide a basis not for interpreting and modeling movement of shallow magma bodies that feed eruptions, but also for detecting intrusive activities that do not result in an eruption [7, 8].

4. Kiska Volcano

Kiska volcano (Fig. 1) is the westernmost historically active volcano in the Aleutian arc. Sequential InSAR images of Kiska show a circular area about 3 km in diameter centered near the summit subsided by as much as 10 cm from 1995 to 2001, mostly during 1999 and 2000 (Fig. 2c). Based on the shallow source depth (< 1 km), the copious amounts of steam during recent eruptions, and recent field reports of vigorous steaming and persistent ground shaking near the summit area, the observed subsidence is attributed to decreased pore-fluid pressure within a shallow hydrothermal system beneath the summit area [9].

5. Augustine Volcano

Augustine volcano (Fig. 1), an 8 by 11 km island, underwent six significant eruptions in the last two centuries: 1812, 1883, 1935, 1963-64, 1976, and 1986. InSAR images show the pyroclastic flows from the 1986 eruption have been experiencing subsidence/compaction at a rate of about 3 cm per year (Fig. 2d) and no sign of significant volcano-wide deformation was observed during 1992-2000. The observed deformation can be used to study the characteristics of the pyroclastic flows [10, 11].

6. Westdahl Volcano

Westdahl volcano (Fig. 1), a young glacier-clad shield volcano was frequently active during the latter half of the 20th century, with documented eruptions in 1964, 1978-79, and 1991-92 [2, 12]. The background level of seismic activity since the last eruption was generally low (about five M < 3 earthquakes per year). InSAR images during 1991-2000 show that Westdahl volcano deflated during its 1991-92 eruption and is re-inflating at a rate that could produce another eruption in the next several years (Fig. 2e). The rates of post-eruptive inflation and co-eruptive deflation are approximated by exponential decay functions with time constants of about 6 years and a few days, respectively. This behavior is consistent with a deep, constant-pressure magma source connected to a shallow reservoir by a magma-filled conduit where the magma flow rate is governed by the pressure gradient between the deep source and the shallow reservoir. This example demonstrates that 1) InSAR is becoming the best tool available for detecting deep, aseismic magma accumulation by measuring broad, subtle deformation of the ground surface, to identify restless volcanoes long before they become active and before seismic and other precursors emerge, and 2) multiple-temporal InSAR images enable constructing a virtual magma plumbing system that can be used to constrain magma accumulation at the shallow reservoir and shed light on the time window of the next eruption [12, 13, 14].

7. Peulik Volcano

Peulik volcano (Fig. 1), a stratovolcano located on the Alaska Peninsula, is known to erupt in 1814 and 1852 [2]. InSAR images that collectively span the time interval from July 1992 to August 2000 reveal that a presumed magma body located 6.6 km beneath the Peulik volcano inflated 0.051 km^3 between October 1996 and September 1998. The average inflation rate of the magma body was about 0.003 km^3/month from October 1996 to September 1997 (Fig. 2f), peaked at 0.005 km^3/month during June 26-October 9, 1997, and dropped to 0.001 km^3/month from October 1997 to September 1998. Deformation before October 1996 or after September 1998 is not significant. An intense earthquake swarm, occurred about 30 km northwest of Peulik from May to October, 1998, around the end of the inflation period. The 1996-98 inflation episode at Peulik confirms that InSAR can be used to detect magma accumulation beneath dormant volcanoes at least several months before other signs of unrest are apparent. This application represents a first step toward understanding the eruption cycle at Peulik and other stratovolcanoes with characteristically long repose periods [15].

8. Seguam Volcano

Seguam volcano (Fig. 1), often referred to Pyre Peak, erupted in 1901, 1927, 1977, and 1992-1993 [2]. InSAR images, spanning various intervals during 1992-2000, document co-eruptive and post-eruptive deformation (Fig. 2g) of the 1992-1993 eruption. A model that combines magma influx, thermoelastic relaxation, and poroelastic effects accounts for the observed deformation. This example demonstrates that spatial and temporal coverage of the InSAR data facilitates revealing dynamic processes within a volcano [10, 16].

9. Makushin Volcano

Makushin volcano, a broad, ice-capped, truncated stratovolcano, is one of the more active volcanoes in the Aleutians, producing at least 17 explosive, relatively small eruptions since the late 1700s [2]. Additional smaller eruptions probably occurred during this period but were unrecorded, either because they occurred when the volcano was obscured by clouds or because the

eruptive products did not extend beyond the volcano's flanks. Several independent InSAR images that each span the time period from October 1993 to September 1995 show evidence of ~7 cm of uplift (Fig. 2h) centered on the volcano's east flank. The uplift was interpreted as pre-eruptive inflation of a small explosive, but unsubstantially reported eruption on January 30, 1995. This example demonstrates that ground deformation of a few cm can be unambiguously identified with InSAR images over a rugged terrain where geometric distortion of radar images is severe [17].

CONCLUSIONS

Satellite InSAR techniques have proven a powerful space-borne geodetic tool to study varied volcanic processes by analyzing surface deformation patterns [1, 3-18]. With the implementation of InSAR technology, volcano monitoring has entered an exciting phase wherein magma accumulation in the middle to upper crust can be observed long before the onset of short-term eruption precursors. Ultimately, more widespread use of InSAR for volcano monitoring could shed light on a part of the eruption cycle - the time period between eruptions when a volcano seems to be doing essentially nothing. This makes InSAR an excellent space-based, long-term volcano monitoring tool. Combining InSAR technique with observations from continuous GPS, gravity, strainmeters, tiltmeters, seismometers and volcanic gas studies will improve our capability to forecast future eruptions and lead to improved volcano hazard assessments and better eruption preparedness.

ACKNOWLEDGMENTS

ERS-1 and ERS-2, Radarsat-1, and JERS-1 SAR images are copyright © 1991-2003 European Space Agency (ESA), Canadian Space Agency (CSA), and Japan Aerospace Exploration Agency (JAXA), respectively, and were provided by ASF and JAXA. The research summarized in the paper was supported by funding from NASA Radarsat Program (NRA-99-OES-10 RADARSAT-0025-0056) and Solid Earth & Natural Hazards Program, USGS contracts O3CRCN0001 and 1434-CR-97-CN-40274, and USGS Volcano Hazards Program. We thank the ASF staff members for their world-class services and special efforts in making the SAR data available to us on a timely basis. We also than J. Freymueller, O. Kwoun, D. Mann, T, Masterlark, V. McConnell, D. Meyer, S. Moran, R. Rykhus, W. Thatcher and many other colleagues for contributions to this research.

References

[1] Lu, Z., R. Fatland, M. Wyss, S. Li, J. Eichelberger, K. Dean, and J. Freymueller, Deformation of New Trident volcano measured by ERS-1 SAR interferometry, Katmai national Park, Alaska, *Geophys. Res. Lett.*, 24:695-698, 1997.

[2] Miller, T.M., R.G. McGimsey, D.H. Richter, J.R. Riehle, C.J. Nye, M.E. Yount, and J.A. Dumoulin, Catalog of the historically active volcanoes of Alaska, *USGS Open-File Report*, 98-582, 1998.

[3] Lu, Z., D. Mann, and J. Freymueller, Satellite radar interferometry measures deformation at Okmok volcano, EOS, 79, 461-468, 1998.

[4] Lu, Z., D. Mann, J. Freymueller, and D. Meyer, Synthetic aperture radar interferometry of Okmok volcano, Alaska: Radar observations, Journal of Geophysical Research, 105, 10791-10806, 2000.

[5] Lu, Z., E. Fielding, M. Patrick, and C. Trautwein, Estimating Lava Volume by Precision Combination of Multiple Baseline Spaceborne and Airborne Interferometric Synthetic Aperture Radar: the 1997 Eruption of Okmok Volcano, Alaska, IEEE Transactions on Geoscience and Remote Sensing, vol. 41, no. 6, 1428-1436, 2003.

[6] Lu, Z., T. Masterlark, and D. Dzurisin, Interferometric Synthetic Aperture Radar (InSAR) Study of Okmok Volcano, Alaska, 1992-2003: Magma Supply Dynamics and Post-emplacement Lava Flow Deformation, Journal of Geophysical Research, submitted, 2004.

[7] Lu, Z., C. Wicks, J. Power, and D. Dzurisin, Ground deformation associated with the March 1996 earthquake swarm at Akutan volcano, Alaska, revealed by satellite radar interferometry, Journal of Geophysical Research, 105, 21,483-21,496, 2000.

[8] Lu, Z., C. Wicks, O. Kwoun, J. Power, and D. Dzurisin, Surface deformation associated with the March 1996 earthquake swarm at Akutan Island, Alaska, revealed by C-band ERS and L-band JERS radar interferometry, Canadian Journal of Remote Sensing, submitted, 2004.

[9] Lu, Z., T. Masterlark, J. Power, D. Dzurisin, and C. Wicks, Subsidence at Kiska volcano, Western Aleutians, Detected by Satellite Radar Interferometry, Geophysical Research Letters, vol. 29, no. 18, 1855, doi:10.1029/2002GL014948, 2002.

[10] Lu, Z., C. Wicks, D. Dzurisin, J. Power, W. Thatcher, and T. Masterlark, Interferometric synthetic aperture radar studies of Alaska volcanoes, Earth Observation Magazine (EOM), vol. 12, No. 3, 8-18, 2003.

[11] Masterlark, T., Z. Lu, and R. Rykhus, Thickness distribution of a cooling pyroclastic flow deposit: Optimization using InSAR, FEMs, and an adaptive mesh algorithm, Journal of Volcanology and Geothermal Research, accepted, 2004.

[12] Lu, Z., R. Rykhus, T. Masterlark, and K. Dean, Mapping recent lava flows at Westdahl volcano, Alaska, using radar and optical satellite imagery, *Remote Sensing of Environment*, 91, 345-353, 2004.

[13] Lu, Z., C. Wicks, D. Dzurisin, W. Thatcher, J. Freymueller, S. McNutt, and D. Mann, Aseismic inflation of Westdahl volcano, Alaska, revealed by satellite radar interferometry, Geophysical Research Letters, 27, 1567-1570, 2000.

[14] Lu, Z., T. Masterlark, D. Dzurisin, R. Rykhus, and C. Wicks, Magma Supply Dynamics at Westdahl Volcano, Alaska, Modeled from Satellite Radar Interferometry, Journal of Geophysical Research, Vol. 108, No. B7, 2354, 10.1029/2002JB002311, 2003.

[15] Lu, Z., C. Wicks, D. Dzurisin J. Power, S. Moran, and W. Thatcher, Magmatic Inflation at a Dormant Stratovolcano: 1996-98 Activity at Mount Peulik Volcano, Alaska, Revealed by Satellite Radar Interferometry, Journal of Geophysical Research, vol. 107, no. B7, 2134, doi:10.1029/2001JB000471, 2002.

[16] Masterlark, T., and Z. Lu, Transient volcano deformation sources imaged with InSAR: Application to Seguam island, Journal of Geophysical Research, J. *Geophys. Res. 109*, B01401, doi:10.1029/2003JB002568, 2004.

[17] Lu, Z., J. Power, V. McConnell, C. Wicks, and D. Dzurisin, Pre-Eruptive Inflation and Surface Interferometric Coherence Characteristics Revealed by Satellite Radar Interferometry at Makushin Volcano, Alaska: 1993 – 2000, Journal of Geophysical Research, vol. 107, no. B11, 2266, doi:10.1029/2001JB000970, 2002.

[18] Lu, Z., and J. Freymueller, Synthetic aperture radar interferometry coherence analysis over Katmai volcano group, Alaska, Journal of Geophysical Research, 103, 29887-29894, 1998.

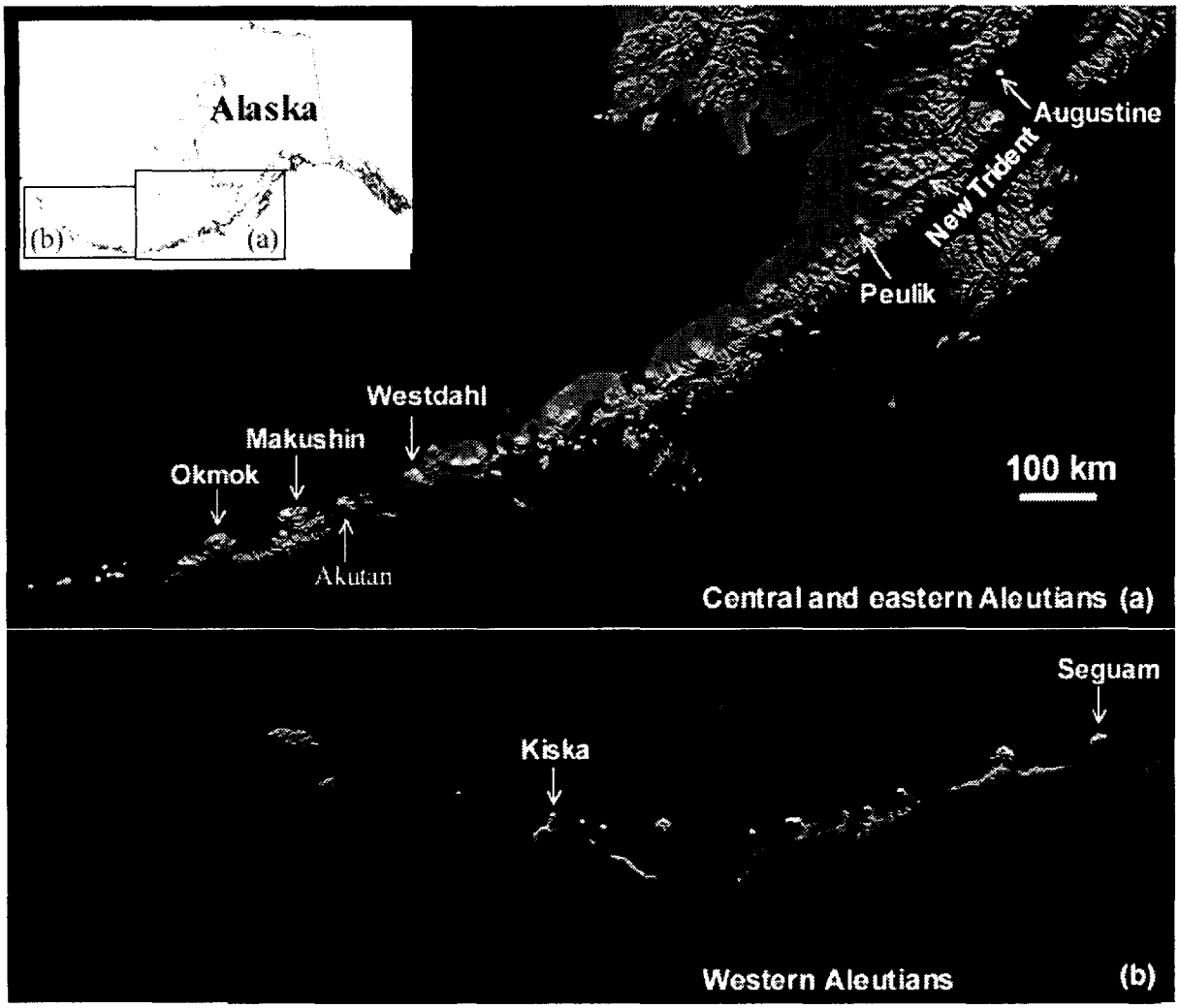

Fig. 1. Location map showing the Alaska volcanoes discussed in this paper. The volcanoes presented in this study spread over the central and eastern Aleutian islands (a) and western Aleutian islands (b).

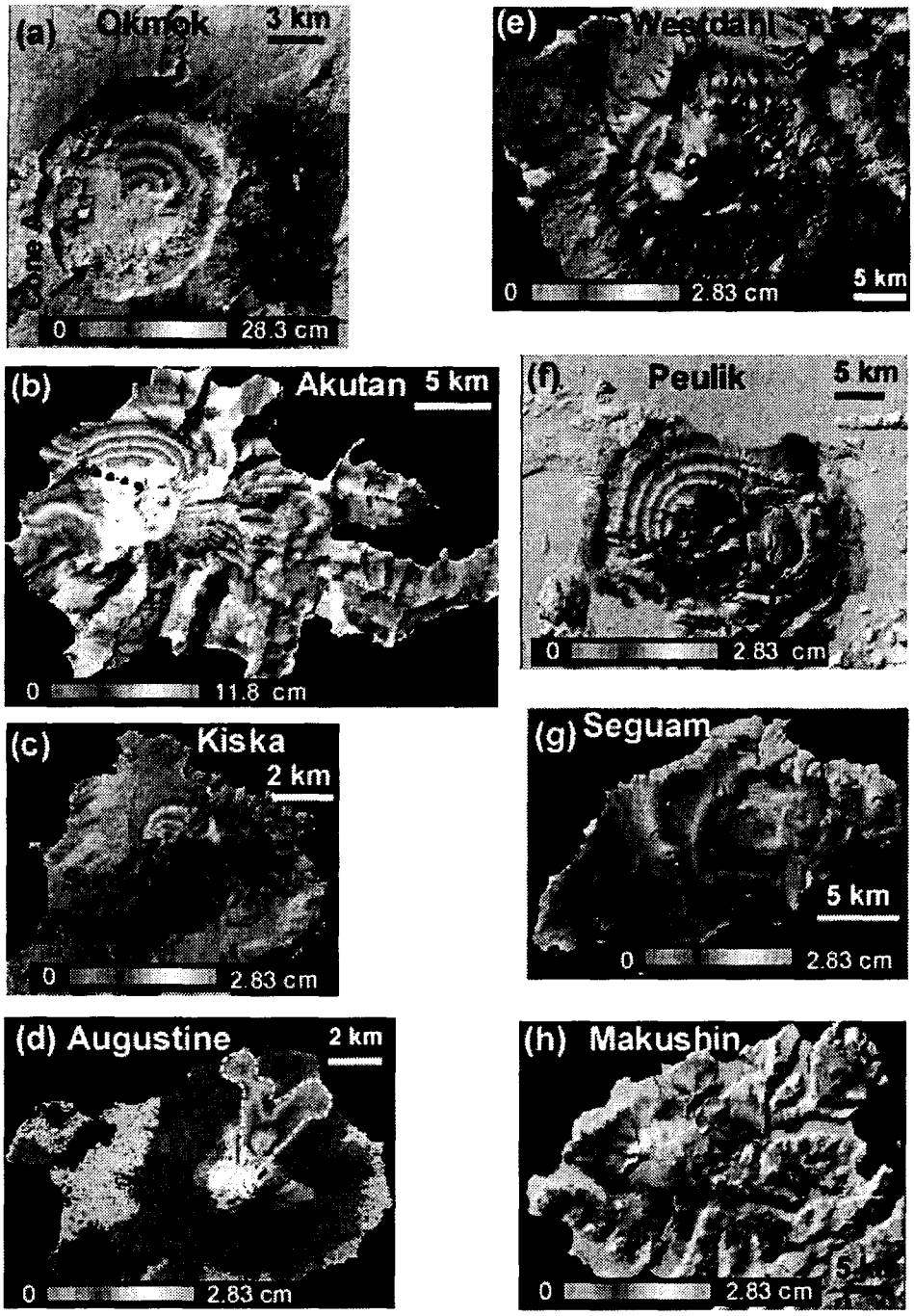

Fig. 2. (a) Deformation interferogram (Oct. 1995 – Sep. 1997), bracketing the Feb. – Apr. 1997 eruption of Okmok volcano. The location of 1997 vent, Cone *A*, is labeled. (b) Deformation interferogram of Akutan volcano, spanning the March 1996 seismic swarm. The dashed line represents a zone of ground cracks created during the 1996 seismic swarm. (c) Deformation interferogram for Kiska volcano during Aug. 1999 and Aug. 2000. (d) Interferogram of Augustine volcano (1992-1993), depicting the deformation associated with the compaction of the 1986 pyroclastic flow deposits outlined by the white dashed line. (e) Aseismic inflation of Westdahl volcano, observed from a 1993-1998 InSAR image. The circle represents the horizontal position of the shallow magma reservoir beneath the Westdahl Peak. (f) Interferogram (Oct. 1996 – Oct. 1997), representing ~17 cm of uplift centered on the southwest flank of Peulik volcano. (g) Interferogram of Makushin volcano, showing about 7 cm inflation associated with a possible eruption in Jan. 1995. (h) Inteferogram of Seguam volcano, showing deformation from Jul. 1999 to Sep. 2000. Interferograms are draped over the DEM shaded relief images and areas without interferometric coherence are uncolored.